Formation of η'(958)-mesic nuclei by the (p,d) reaction

Hideko Nagahiro,[1] Daisuke Jido,[2,3] Hiroyuki Fujioka,[4] Kenta Itahashi,[5] and Satoru Hirenzaki[1]

[1]*Department of Physics, Nara Women's University, Nara 630-8506, Japan*

[2]*Yukawa Institute for Theoretical Physics, Kyoto University, Kyoto 606-8502, Japan*

[3]*J-PARC Branch, KEK Theory Center, Institute of Particle and Nuclear Studies, High Energy Accelerator Research Organization (KEK), Ibaraki 319-1106, Japan*

[4]*Division of Physics and Astronomy, Kyoto University, Kyoto 606-8502, Japan*

[5]*Nishina Center for Accelerator-Based Science, RIKEN, 2-1 Hirosawa, Wako, Saitama 351-0198, Japan*

(Received 14 November 2012; published 2 April 2013)

We calculate theoretically the formation spectra of η'(958)-nucleus systems in the (p,d) reaction for the investigation of in-medium modification of the η' mass. We show comprehensive numerical calculations based on a simple form of the η' optical potential in nuclei with various potential depths. We conclude that one finds evidence of a possible attractive interaction between η' and the nucleus as a peak structure appearing around the η' threshold in light nuclei such as ^{11}C, when the attractive potential is stronger than 100 MeV and the absorption width is of order 40 MeV or less. Spectroscopy of the (p,d) reaction is expected to be performed experimentally at existing facilities, such as GSI. We also estimate the contributions from the ω and ϕ mesons, which have masses close to the η' meson, concluding that the observation of the peak structure of the η'-mesic nuclei is not disturbed, although their contributions may not be small.

DOI: 10.1103/PhysRevC.87.045201 PACS number(s): 21.85.+d, 21.65.Jk, 11.30.Rd, 25.40.Ve

I. INTRODUCTION

The η'(958) meson is an interesting and important particle because of its exceptionally large mass and connection to the $U_A(1)$ problem [1]. According to the symmetry pattern of the quark sector in QCD, the η' meson would be one of the Nambu-Goldstone bosons associated with the spontaneous breakdown of the $U(3)_L \times U(3)_R$ chiral symmetry to the $U_V(3)$ flavor symmetry. In the real world, however, gluon dynamics plays an important role, and the η' meson acquires its peculiarly larger mass than those of the other pseudoscalar mesons, π, K, and η, through the quantum anomaly effect of nonperturbative gluon dynamics [2,3] which induces the nontrivial vacuum structure of QCD [4]. The mass generation of the η' meson is considered to be a result of the interplay of quark symmetry and gluon dynamics. The η' meson at finite density has been discussed for a long time [5–9] and the possible formation spectra of the η'-mesic nuclei was first investigated in Ref. [10] with the (γ, p) reaction.

Recently, there have been two important developments in theoretical [11] and experimental [12] points of view for the study of the η' mass at finite density. In Refs. [11,13,14], it has been pointed out theoretically that the anomaly effect can contribute to the η' mass only with the presence of the spontaneous and/or explicit breaking of chiral symmetry. This is because the chiral singlet gluon current cannot couple to the chiral pseudoscalar mesonic state without the chiral symmetry breaking.[1] Thus, even if density dependence of the $U_A(1)$ anomaly effect is irrelevant or negligible, a relatively large mass reduction ($\sim$100 MeV) of the η' meson is expected at nuclear density due to the partial restoration of chiral symmetry. In Fig. 1 we show a schematic view of the pseudoscalar meson spectra in various chiral symmetry breaking patterns.

Meanwhile, in Ref. [12], it has been reported that the experimental observation of the η'-nuclear bound states predicted in Refs. [10,15] is considered to be possible. This observation will help us much to understand the η' mass generation mechanism quantitatively. In a meson-nucleus bound system such as deeply bound pionic atoms [16], because it is guaranteed that the meson inhabits the nucleus, it is unnecessary to remove in-vacuum contributions from the spectrum. The fact that the bound states have definite quantum numbers is favorable for extracting fundamental quantities, since detailed spectroscopy enables us to investigate selectively the contents of the in-medium meson self-energy [16–18]. Since so far there have been no observations of the η' meson bound in nuclei, it is extremely desirable to search for experimental signals of η' bound states in nuclei as a first step to the detailed investigation of the in-medium η' meson properties.

Thus, in this article, we show the comprehensive calculation of the formation spectra of the η' meson-nucleus systems in the (p,d) reaction [12] based on the latest theoretical considerations of η' property in nuclei [11,19]. The numerical results shown here are important both to give theoretical support and predictions to the planned experiment in Ref. [12], and to make it possible to deduce clearly the η' property in nuclei from the experimental data.

We should stress that this η' mass reduction mechanism has a unique feature [11]. In usual meson-nuclear systems, attractive interactions induced by many-body effects unavoidably accompany comparably large absorptions. This is because attractive interaction and absorption process are originated by the same hadronic many-body effects. This implies that the bound states have a comparable absorption width with the level

[1]For the flavor SU(2), in which the strange quark is infinitely heavy, nontrivial topological sectors can contribute differently to two-point functions of η and η' even in the chiral symmetric limit. Thus η and η' do not degenerate in the chiral restoration limit [13].

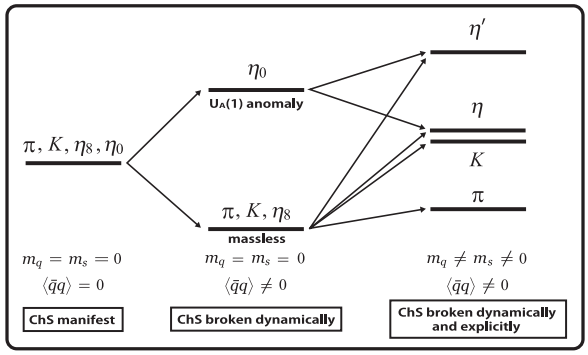

FIG. 1. Light pseudoscalar meson spectrum in the various patterns of the SU(3) chiral symmetry breaking. In the left the chiral symmetry is manifest with neither explicit nor dynamical breaking. All the pseudoscalar mesons have a common mass. In the middle, chiral symmetry is dynamically broken in the chiral limit. The octet pseudoscalar mesons are identified as the Nambu-Goldstone bosons associated with the symmetry breaking. In the right chiral symmetry is broken dynamically by the quark condensate and explicitly by finite quark masses.

spacing. In the present case, however, since the suppression of the $U_A(1)$ anomaly effect in nuclear medium induces the attractive interaction to the in-medium η' meson, the influence acts selectively on the η' meson and, thus, it hardly induces inelastic transitions of the η' meson into lighter mesons, although other many-body effects can introduce nuclear absorptions of the η' meson. Consequently the η' meson bound state is expected to have a larger binding energy with a smaller width [11]. This feature is supported by the theoretical optical potential evaluated in Ref. [19] based on the theoretical $\eta' N$ scattering amplitude [20].

As for other experimental information obtained so far, it has been reported that a strong reduction of the η' mass, at least 200 MeV, is necessary to explain the two-pion correlation in Au + Au collisions at the Relativistic Heavy Ion Collider (RHIC) [21]. In contrast, a low-energy η' production experiment with pp collision has suggested a relatively smaller scattering length of the s-wave η'-proton interaction, $|\mathrm{Re}\ a_{\eta' p}| < 0.8$ fm [22] and $|a_{\eta' p}| \sim 0.1$ fm [23], which corresponds to from several to tens of MeV mass reduction at nuclear saturation density estimated under the linear density approximation. Transparency ratios for η' mesons have been measured for different nuclei by the CBELSA/TAPS Collaboration [24,25]. An absorption width of the η' meson at saturation density as small as 15–25 MeV has been found. Within the experimental uncertainties this width seems to be almost independent of the η' momentum. Theoretically, the formation spectra of the η' mesic nuclei were calculated first in Ref. [10]. Nambu–Jona-Lasinio (NJL) model calculations suggested around 150 MeV mass reduction of the η' meson at the saturation density [15,26]. The theoretical model of Refs. [19,20] shows, however, that the existence of the strong attraction is not consistent with the latest data of the small scattering length [23].

This article is organized as follows. In Sec. II, we give the formulation to calculate the formation spectra of the η'-nucleus bound states. The calculated spectra are shown in Sec. III. We also show the formation spectra with various optical potential cases in the Appendix. Finally, we will devote Sec. IV to conclude this article.

II. FORMULATION OF η'-NUCLEUS BOUND STATE FORMATION

In this article, we consider the (p,d) reaction for the formation of the η'-mesic nuclei, which can be performed at existing facilities like GSI [12]. Missing-mass spectroscopy is considered here and it has been proven to be a powerful tool for the formation of the meson bound states [27]. In this spectroscopy, one observes only an emitted particle in a final state, and obtains the double differential cross section $d^2\sigma/d\Omega dE$ as a function of the energy of the η'-nucleus system which is uniquely determined by the emitted particle energy by means of the energy conservation law.

To evaluate the formation cross section, we use the Green's function method [28,29]. In this method, the reaction cross section is assumed to be separated into the nuclear response function $R(E)$ and the elementary cross section of the $pn \to d\eta'$ process with the impulse approximation:

$$\left(\frac{d^2\sigma}{d\Omega dE}\right)_{A(p,d)(A-1)\otimes\eta'} = \left(\frac{d\sigma}{d\Omega}\right)^{\mathrm{lab}}_{n(p,d)\eta'} \times R(E), \qquad (1)$$

where the nuclear response function $R(E)$ is given in terms of the in-medium Green's function $G(E)$ as

$$R(E) = -\frac{1}{\pi}\,\mathrm{Im}\sum_f \int d\mathbf{r}\, d\mathbf{r}'\, \mathcal{T}_f^\dagger(\mathbf{r}) G(E;\mathbf{r},\mathbf{r}')\mathcal{T}_f(\mathbf{r}'). \qquad (2)$$

Here, the summation is inclusively taken over all possible final states. The amplitude $\mathcal{T}_f$ describes the transition of the incident proton to a neutron hole and the outgoing deuteron:

$$\mathcal{T}_f(\mathbf{r}) = \chi_d^*(\mathbf{r})\left[Y^*_{l_{\eta'}}(\hat{r}) \otimes \psi_{j_n}(\mathbf{r})\right]_{JM} \chi_p(\mathbf{r}) \qquad (3)$$

with the neutron hole wave function ψ_{j_n}, the distorted waves of the proton and the ejected deuteron χ_p and χ_d, and the η' angular wave function $Y_{l_{\eta'}}(\hat{r})$. For the neutron hole, we use the harmonic oscillator wave function for simplicity. The Green's function $G(E)$ contains the η'-nucleus optical potential in the Hamiltonian as

$$G(E;\mathbf{r},\mathbf{r}') = \langle n^{-1}|\phi_{\eta'}(\mathbf{r})\frac{1}{E - H_{\eta'} + i\epsilon}\phi^\dagger_{\eta'}(\mathbf{r}')|n^{-1}\rangle \qquad (4)$$

where $\phi^\dagger_{\eta'}$ is the η' creation operator and $|n^{-1}\rangle$ is the neutron hole state. The elementary cross section in the laboratory frame in Eq. (1) was evaluated to be 30 μb/sr at the proton kinetic energy $T_p = 2.5$ GeV in Refs. [12,30]. The Green's function $G(E,\mathbf{r},\mathbf{r}')$ can be obtained by solving the Klein-Gordon equation with the appropriate boundary condition. Thus, the Green's function represents both the η' meson scattering states and bound states together with the decay modes which are expressed in the imaginary part of the potential. The imaginary

part of the Green's function, or the spectral function, represents the coupling strength of the η' meson to each intermediate state as a function of the energy of the η' meson. If there is a quasibound state of the η' meson, the spectral function has a peak structure at the corresponding energy. This can be seen in the formation spectra as a signal of the bound state.

In this article, to discuss the observation feasibilities, we go through various cases with different optical potentials for the η'-nucleus system. If the mass reduction as expected by the NJL calculation takes place in nuclear matter, we can translate its effect into a potential form. The optical potential $U_{\eta'}(r)$ can be written as

$$U_{\eta'}(r) = V(r) + iW(r), \tag{5}$$

where V and W denote the real and imaginary parts of the optical potential, respectively. The mass term in the Klein-Gordon equation for the η' meson at finite density can be written as

$$\begin{aligned} m_{\eta'}^2 \to m_{\eta'}^2(\rho) &= [m_{\eta'} + \Delta m(\rho)]^2 \\ &\sim m_{\eta'}^2 + 2m_{\eta'}\Delta m_{\eta'}(\rho), \end{aligned} \tag{6}$$

where $m_{\eta'}$ is the mass of the η' meson in vacuum and $m_{\eta'}(\rho)$ the mass at finite density ρ. The mass shift $\Delta m_{\eta'}(\rho)$ is defined as $\Delta m_{\eta'}(\rho) = m_{\eta'}(\rho) - m_{\eta'}$. Thus, we can interpret the mass shift $\Delta m_{\eta'}(\rho)$ as the strength of the real part of the optical potential

$$V(r) = \Delta m_{\eta'}(\rho_0)\frac{\rho(r)}{\rho_0} \equiv V_0\frac{\rho(r)}{\rho_0} \tag{7}$$

in the Klein-Gordon equation using the mass shift at normal saturation density ρ_0. Here we assume the nuclear density distribution $\rho(r)$ to be of an empirical Woods-Saxon form as

$$\rho(r) = \frac{\rho_N}{1 + \exp(\frac{r-R}{a})}, \tag{8}$$

where $R = 1.18A^{\frac{1}{3}} - 0.48$ fm, $a = 0.5$ fm with nuclear mass number A, and ρ_N a normalization factor such that $\int d^3r\rho(r) = A$. In the following sections, we show the (p,d) spectra with potential depth from $V_0 = 0$ to -200 MeV and $W_0 = -5$ to -20 MeV to discuss the observation feasibility, where W_0 is the strength of the imaginary part of the optical potential at ρ_0.

Alternatively, we also use the theoretical optical potentials for the η'-nucleus system obtained in Ref. [19] by imposing several theoretical $\eta' N$ scattering lengths [20] and using the standard many-body theory. There the two-body absorption of the η' meson in a nucleus together with the one-body absorption has been evaluated so that we can decompose the spectra into the different final states by using the Green's function method as discussed below.

We obtain the in-medium Green's function by solving the Klein-Gordon equation with the optical potential $U_{\eta'}$ in Eq. (5) with the appropriate boundary condition and use it to evaluate the nuclear response function $R(E)$ in Eq. (1).

We estimate the flux loss of the injected proton and the ejected deuteron due to the elastic and quasielastic scattering and/or absorption processes by the target and daughter nuclei. To estimate the attenuation probabilities, we approximate the distorted waves of the incoming proton χ_p and the outgoing deuteron χ_d as

$$\chi_d^*(\boldsymbol{r})\chi_p(\boldsymbol{r}) = \exp[i\boldsymbol{q}\cdot\boldsymbol{r}]F(\boldsymbol{r}), \tag{9}$$

with the momentum transfer between proton and deuteron $\boldsymbol{q} = \boldsymbol{p}_p - \boldsymbol{p}_d$ and the distortion factor $F(\boldsymbol{r})$ evaluated by

$$\begin{aligned} F(\boldsymbol{r}) = \exp\Bigg[&-\frac{1}{2}\sigma_{pN}\int_{-\infty}^{z} dz'\rho_A(z',b) \\ &-\frac{1}{2}\sigma_{dN}\int_{z}^{\infty} dz'\rho_{A-1}(z',b)\Bigg]. \end{aligned} \tag{10}$$

Here σ_{pN} and σ_{dN} are the proton-nucleon and deuteron-nucleon total cross sections, respectively, which contain both the elastic and inelastic processes. The values of the total cross sections are taken from Ref. [31]. $\rho_A(z,b)$ is the density distribution function for the nucleus with the mass number A in cylindrical coordinates.

The calculation of the formation spectra is done separately for each subcomponent of the η'-mesic nuclei labeled by $(n\ell_j)_n^{-1} \otimes \ell_{\eta'}$, which means a configuration of a neutron-hole in the ℓ orbit with the total spin j and the principal quantum number n in the daughter nucleus and an η' meson in the $\ell_{\eta'}$ orbit. The total formation spectra are obtained by summing up these subcomponents, taking into account the difference of the separation energies for the different neutron-hole states.

The energy of the emitted deuteron determines the energy of the η'-nucleus system uniquely. We show the calculated spectra as functions of the excitation energy $E_{\rm ex} - E_0$ defined as

$$E_{\rm ex} - E_0 = -B_{\eta'} + [S_n(j_n) - S_n(\text{ground})], \tag{11}$$

where $B_{\eta'}$ is the η' binding energy and $S_n(j_n)$ the neutron separation energy from the neutron single-particle level j_n. S_n(ground) indicates the separation energy from the neutron level corresponding to the ground state of the daughter nucleus. E_0 is the η' production threshold energy.

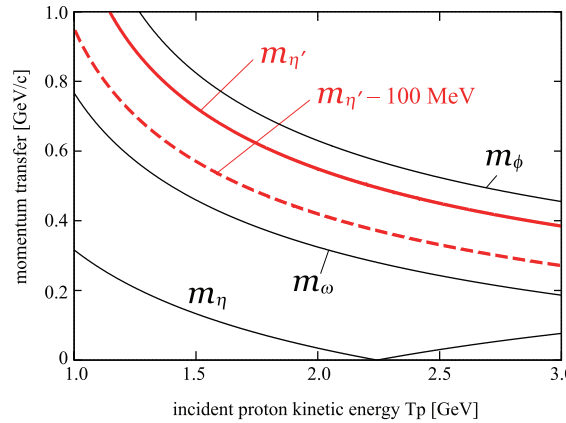

FIG. 2. (Color online) Momentum transfer of the ^{12}C(p,d) reactions as functions of the incident proton kinetic energy T_p. The thick solid and dashed lines correspond to η' meson production with binding energies of 0 and 100 MeV. Thin solid lines correspond to η, ω, and ϕ meson productions with a binding energy of 0 MeV, as indicated in the figure.

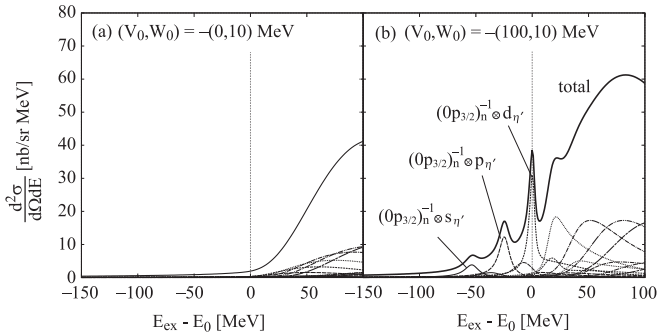

FIG. 3. Calculated spectrum of the $^{12}C(p,d)^{11}C\otimes\eta'$ reaction for the formation of η'-nucleus systems with proton kinetic energy $T_p = 2.5$ GeV and deuteron angle $\theta_d = 0^\circ$ as a function of the excited energy E_{ex}. E_0 is the η' production threshold. The depths of the η'-nucleus optical potential are (a) $(V_0, W_0) = -(0, 10)$ MeV, and (b) $(V_0, W_0) = -(100, 10)$ MeV. The thick solid line shows the total spectrum and dashed lines indicate subcomponents. The neutron-hole states are indicated as $(n\ell_j)_n^{-1}$ and the η' states as $\ell_{\eta'}$.

The widths of the hole states are taken into account in the present calculation. The width of the neutron-hole states in ^{11}C have been estimated to be $\Gamma((0s_{1/2})^{-1}) = 12.1$ MeV for the excited state and $\Gamma((0p_{3/2})^{-1}) = 0$ MeV for the ground state by using the data in Ref. [32]. As for ^{39}Ca, we use $\Gamma = 7.7$ MeV $[(1s_{1/2})^{-1}]$, 3.7 MeV $[(0d_{5/2})^{-1}]$, 21.6 MeV $[(0p_{3/2,1/2})^{-1}]$, and 30.6 MeV $[(0s_{1/2})^{-1}]$ estimated from the data in Ref. [33], considering the width of the ground state $(0d_{3/2})^{-1}$ to be 0 and assuming the same widths for neutron-hole states as those of proton holes.

In the Green's function method [28], one can separately calculate each contribution to the spectrum coming from the different η' processes. On the prescription of Ref. [28], we rewrite equivalently the imaginary part of the Green's function of η' as

$$\mathrm{Im}\,G = (1 + G^\dagger U_{\eta'}^\dagger)\,\mathrm{Im}\,G_0(1 + U_{\eta'}G) + G^\dagger\,\mathrm{Im}\,U_{\eta'}G, \tag{12}$$

where G and G_0 denote the full and free Green's functions for η' and $U_{\eta'}$ is the η'-nucleus optical potential. We abbreviate the integral symbols in Eq. (12). The first term of the right-hand side of Eq. (12) represents the contribution from the escape η' from the daughter nucleus and the second term describes the conversion process caused by the η' absorption into the nucleus. By evaluating only the conversion part, we obtain spectra associated with decays (or absorptions) of the η' mesons in the nucleus, which correspond to the coincident measurements in real experiments.

III. NUMERICAL RESULTS

First, we show in Fig. 2 the momentum transfer of the (p,d) reactions for the formation of the η' meson. We also show those for the η, ω, and ϕ meson production cases. Those mesons, which have relatively closer masses to that of η', can contribute to the (p,d) spectrum in the same energy region [15]. We find that the recoilless condition can be satisfied only for the η production case in this energy region. For the η' production case, the recoilless condition is never satisfied even for the η' bound states with the binding energy of 100 MeV. The momentum transfer at $T_p = 2.5$ GeV, which is the energy considered in Ref. [12], is around 400–500 MeV/c, and thus various contributions of $(n\ell_j)_n^{-1}\otimes\ell_{\eta'}$ will contribute to the (p,d) spectrum.

We show the calculated formation spectra of an η'-nucleus system for the ^{12}C target case with the potential strength $(V_0, W_0) = -(0, 10)$ and $-(100, 10)$ MeV cases in Fig. 3. As we can see from the figure, the existence of the attractive interaction and bound states can be seen as the peak structures in the (p,d) spectrum. We find that there is a clear difference between the cases with attractive and nonattractive potentials.

In Fig. 4, we show the effects of the absorption interaction by varying the strength of the imaginary part W_0 of the optical potential. We can see the clear peaks corresponding to bound states in the s, p and d states, although the width of each peak becomes wider as W_0 is increased. We also find that there are peak structures in the $f_{\eta'}$-wave component just above the threshold $(E_{ex} - E_0 = 0)$ owing to the so-called threshold enhancement. While there are no bound states in the $f_{\eta'}$ state of η', the attractive η'-nucleus interaction pulls

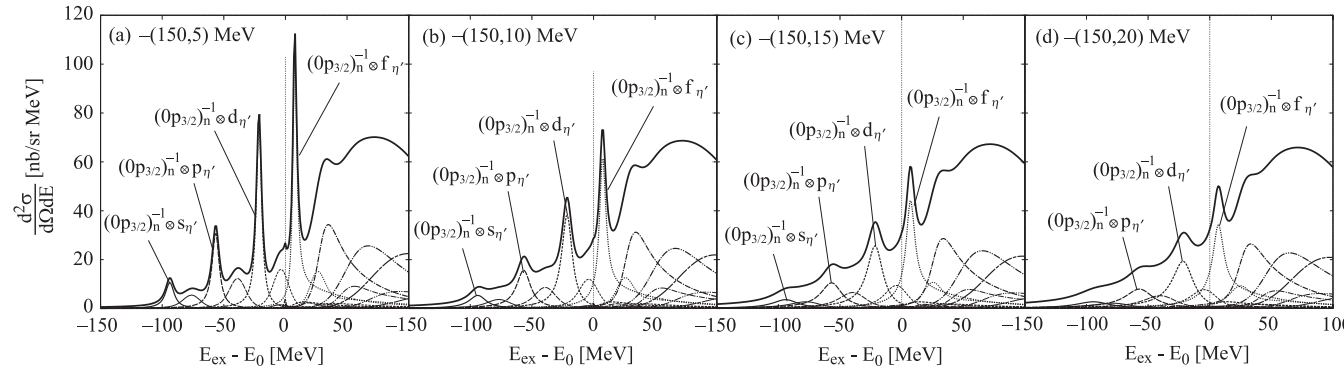

FIG. 4. Calculated spectra of the $^{12}C(p,d)^{11}C\otimes\eta'$ reaction for the formation of η'-nucleus systems with proton kinetic energy $T_p = 2.5$ GeV and deuteron angle $\theta_d = 0^\circ$ as functions of the excited energy E_{ex}. E_0 is the η' production threshold. The η'-nucleus optical potentials are (a) $(V_0, W_0) = -(150, 5)$ MeV, (b) $-(150, 10)$ MeV, (c) $-(150, 15)$ MeV, and (d) $-(150, 20)$ MeV. The thick solid lines show the total spectra and dashed lines indicate subcomponents. The neutron-hole states are indicated as $(n\ell_j)_n^{-1}$ and the η' states as $\ell_{\eta'}$.

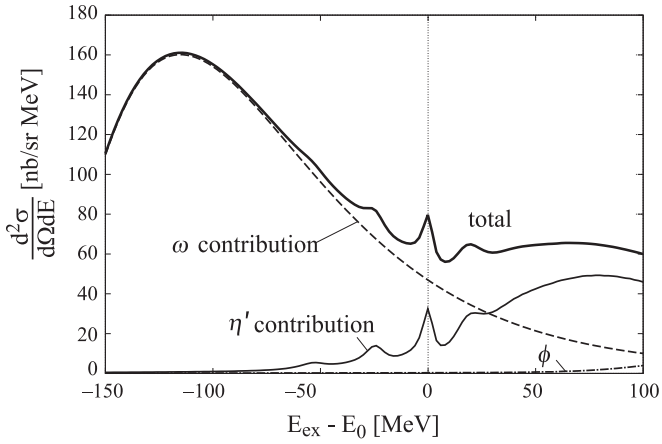

FIG. 5. Calculated spectra of the ^{12}C$(p,d)^{11}$C $\otimes\,\eta'$, ^{12}C$(p,d)^{11}$C $\otimes\,\omega$, and ^{12}C$(p,d)^{11}$C $\otimes\,\phi$ reactions for the formation of meson-nucleus systems with proton kinetic energy $T_p = 2.6$ GeV and deuteron angle $\theta_d = 0^\circ$ as functions of the excited energy $E_{\rm ex}$. E_0 is the η' production threshold. The η'-nucleus optical potential is $(V_0, W_0) = -(100, 10)$ MeV, the ω-nucleus optical potential is $(V_0, W_0) = -(-42.8, 19.5)$ MeV [34], and the ϕ-nucleus optical potential is $(V_0, W_0) = -(30, 10)$ MeV [35–38]. The thin solid line shows the η' production, and the dashed and dot-dashed lines indicate the ω and ϕ meson productions. The contributions of mesonic states with partial waves up to $\ell = 6$ for each meson are included in the calculation.

this low-energy scattering wave of η' closer to the daughter nucleus, enhancing its overlap with the nucleon wave functions and consequently producing a larger cross section. Therefore, we can consider this enhancement to give an indication of the attractive η'-nucleus interaction if observed. We find that, even in a large imaginary case of $-(150, 20)$ MeV, we can see a clear peak corresponding to this threshold enhancement, indicating the attractive nature of the η'-nucleus optical potential. In the Appendix, we show various cases of the strength of the real optical potentials to see the experimental feasibility systematically. We find that, in the weak attraction $V_0 = -50$ MeV case, we cannot see peak structures with larger absorption $|W_0| \gtrsim 15$ MeV, while in the strong attraction $|V_0| \gtrsim 100$ MeV case we can see clear peaks even in the large absorption $W_0 = -20$ MeV, which corresponds to the absorption width $\Gamma = 40$ MeV.

The contributions from other meson production processes are shown in Fig. 5. Because we are considering the inclusive reaction in this article, the productions of other mesons having close masses also contribute to the spectra of the (p,d) reaction in addition to the formation of the η'-mesic nuclei. Here, we take the contributions from the ω and ϕ mesons into account in Fig. 5. The incident proton kinetic energy is set to be $T_p = 2.6$ GeV. The ϕ-nucleus interaction is taken as $V_\phi = -(30 + 10i)\rho(r)/\rho_0$ MeV which corresponds to the 3% mass reduction of the ϕ meson at normal saturation density. The imaginary part of the optical potential has been estimated by using the chiral unitary approach, and $W_0 = -10$ MeV is used here as in Ref. [35]. The elementary cross section of $pn \to d\phi$ is estimated as $(d\sigma/d\Omega)^{\rm lab} = 13.5\ \mu$b/sr by using the experimental data [39]. As we can see in the figure, the contribution from the ϕ meson is negligibly small owing to the large momentum transfer for the ϕ meson production.

In contrast to the ϕ meson, we find that the ω meson production gives larger contribution to the η' bound region. Although it is still unknown whether the ω-nucleus interaction is attractive or repulsive, we consider the case that the ω-nucleus optical potential is repulsive as $V_\omega = -(-42.8 + 19.5i)\rho(r)/\rho_0$ MeV [34,40] because in the repulsive case the quasifree ω contribution above the ω production threshold is enhanced and then it overlaps the η' bound region [15]. The elementary cross section of $pn \to d\omega$ in the laboratory frame with $T_p = 2.6$ GeV is estimated as 27 μb/sr by using the experimental data [41]. As shown in Fig. 5, although the contribution of the quasifree ω is large, the strength of the tail around the η' threshold, where we can see the clear peak

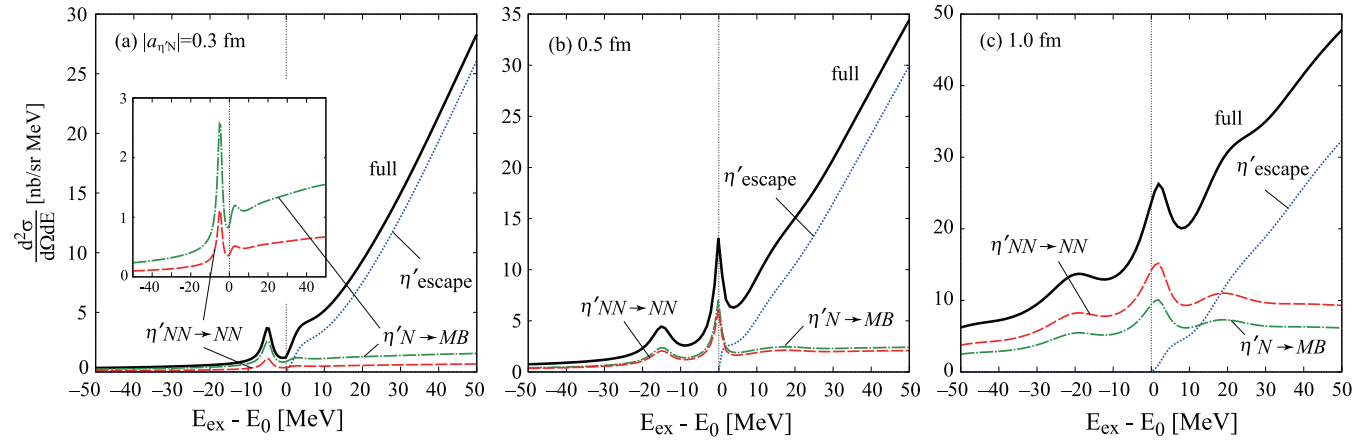

FIG. 6. (Color online) Calculated spectra of the ^{12}C$(p,d)^{11}$C $\otimes\,\eta'$ reaction for the formation of η'-nucleus systems with proton kinetic energy $T_p = 2.5$ GeV and deuteron angle $\theta_d = 0^\circ$ as functions of the excited energy $E_{\rm ex}$. E_0 is the η' production threshold. The η'-nucleus optical potentials are evaluated in Ref. [19], which correspond to the η' scattering lengths $|a_{\eta' p}| =$ (a) 0.3, (b) 0.5, and (c) 1.0 fm, respectively. The thick solid lines show the total spectra and dashed lines show subcomponents as indicated in the figure. The inset figure in panel (a) shows the structure of the subcomponents in closeup.

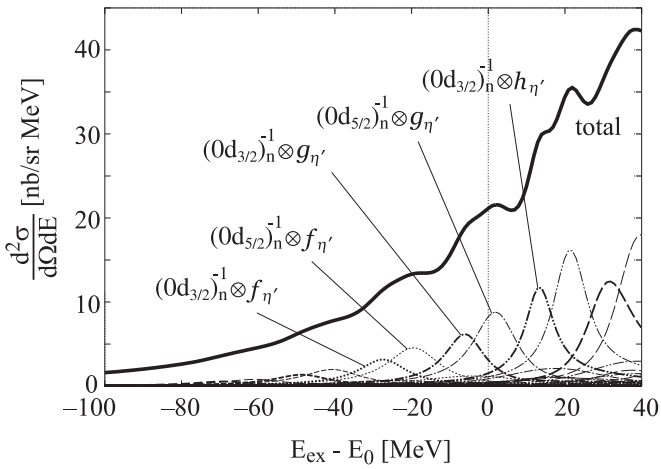

FIG. 7. Calculated spectra of the ^{40}Ca$(p,d)^{39}$Ca $\otimes\,\eta'$ reaction for the formation of η'-nucleus systems with proton kinetic energy T_p = 2.5 GeV and deuteron angle $\theta_d = 0^\circ$ as functions of the excited energy E_{ex}. E_0 is the η' production threshold. The η'-nucleus optical potential is $(V_0, W_0) = -(100, 10)$ MeV. The thick solid lines show the total spectra and dashed lines indicate subcomponents. The neutron-hole states are indicated as $(n\ell_j)_n^{-1}$ and the η' states as $\ell_{\eta'}$.

of η', is of the same order of the η' signal and does not have any structure there. Therefore, we can expect to observe the peak structure of η' even if there is a quasielastic ω contribution.

In Fig. 6, we show the results calculated with the theoretical optical potentials in Ref. [19]. The potential parameters used here correspond to $\eta' N$ scattering lengths of $|a_{\eta' N}| = 0.3$, 0.5, and 1.0 fm, respectively [19,20]. In these figures, we show only the η' contribution as in Figs. 3 and 4. As shown in Fig. 6, we decompose the total spectrum for each case into three parts: the contribution from the η'-escape process and two conversion parts of the one-body absorption $\eta' N \to MB$ (where M denotes a meson and B a baryon which are included in the coupled-channel calculation in Ref. [20]) and two-body absorption $\eta' NN \to NN$. The spectra with coincident observations of a nucleon pair associated with the two-body absorption of η' are shown by the dashed lines and those of a meson-baryon (mostly ηN or πN) pair by the dot-dashed lines. These conversion spectra shown in Fig. 6 give useful information for coincident measurements of the decay particles from the η'-bound states, which could reduce the large background estimated in Ref. [12].

We show the results with the heavier ^{40}Ca target in Fig. 7. In some cases, a larger target is more suitable because there are more bound states. In the case of the η'-mesic nuclei formation by the (p,d) reaction, however, the bound state peaks overlap each other because of the smaller level spacing than the ^{12}C case. Therefore, we conclude that a smaller target like ^{12}C is better suited for the η'-mesic nuclei formation.

IV. CONCLUSIONS

We have calculated the formation spectra of the $\eta'(958)$-nucleus systems for the (p,d) reaction. The kinetic energy of the incident proton beam is set to be T_p = 2.5–2.6 GeV, which can be reached at existing facilities like GSI [12]. We have shown the numerical results for various strengths of the η'-nucleus optical potentials from $V_0 = 0$ to -200 MeV and $W_0 = -5$ to -20 MeV as well as the no-attraction case$(V_0, W_0) = -(0, 10)$ MeV. We find that, in the strong attraction case $|V_0| \gtrsim 100$ MeV, which is the expected strength of the attraction by the NJL calculation, we can see clear peaks around the η' production threshold even with the large absorption case $W_0 = -20$ MeV. In some cases, the peaks around the threshold do not indicate the existence of the bound states, but show the so-called threshold enhancements which are also consequences of the attractive nature of the η'-nucleus interaction. The robustness of the appearance of the peak structure around the threshold for an attractive interaction, which is independent of the detail of the model parameters within the range of the present consideration, is an interesting and important finding of this study. We conclude that we can see a clear signal of the possible attractive potential of the η'-nucleus system by the (p,d) reaction with ^{12}C target. The conversion spectra accompanied by different absorption processes of η' in nuclei are discussed, which give useful information to the coincident measurements of the decay particles from the η' bound states.

We also have looked at the contributions from other meson productions whose mass is close to that of η'. Although they must be one of the sources of the background, the contributions are almost structureless and then do not disturb the peak observation of η'. We have discussed the heavier target nucleus case as well, because it is often said that a larger target is more suitable to make a bound state. We find that, however, in the present case a relatively light nucleus such as ^{12}C, likely to have not many but a few bound states, is suited to observe peaks in the formation spectra.

So far, a relatively small scattering length of the η'-nucleon has been reported [22,23], although its sign is still unknown. If such a small scattering length is a consequence of a weak attraction, it will be difficult to observe the η'-nucleus bound states by using the proposed method here. In such a case, we have to develop an advanced understanding of such a small η'-nucleon interaction from the microscopic and fundamental points of view.

In contrast, the transparency ratios of the η' meson have been measured by the CBELSA/TAPS Collaboration [24,25] and suggest remarkably small absorption width of the η' meson in nuclear medium as compared to other mesons such as η or ω, which is consistent with a scenario for the fate of η' in finite density discussed in Ref. [11].

In any case, an experimental search for bound η' in nuclei would provide important information on the properties of η'. We believe that the present theoretical results are very important for such experimental activities to obtain deeper insight into the meson mass spectrum.

ACKNOWLEDGMENTS

We appreciate the useful discussions with E. Oset, A. Ramos, V. Metag, and M. Nanova. This work is

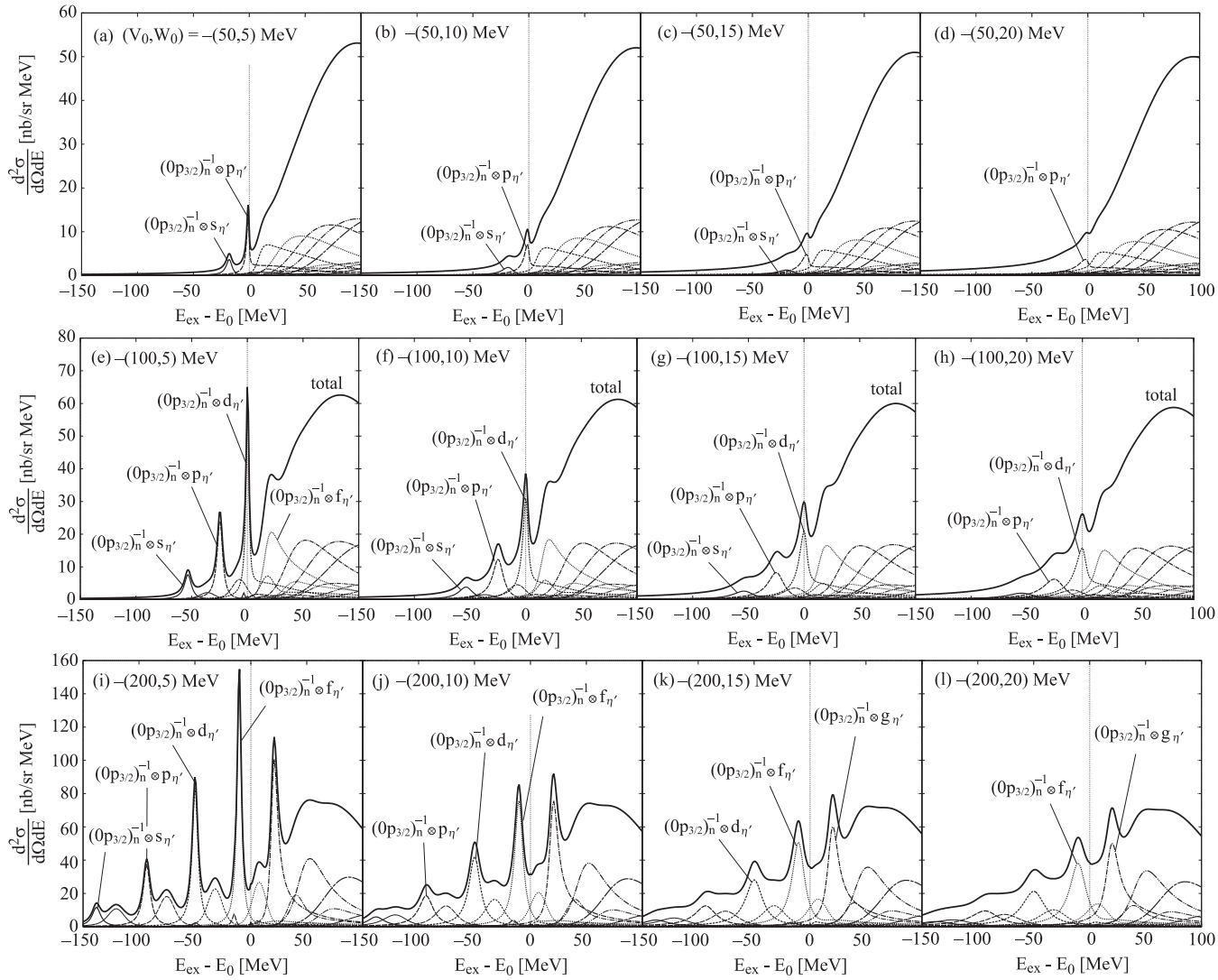

FIG. 8. Calculated spectra of the ^{12}C$(p,d)^{11}$C $\otimes\,\eta'$ reaction for the formation of η'-nucleus systems with proton kinetic energy $T_p = 2.5$ GeV and deuteron angle $\theta_d = 0^\circ$ as functions of the excited energy $E_{\rm ex}$. E_0 is the η' production threshold. Various combinations of the potential strength are considered within the range of $V_0 = -50$–200 MeV and $W_0 = -5$–20 MeV as indicated in the figure. The thick solid lines show the total spectra and dashed lines indicate subcomponents. The neutron-hole states are indicated as $(n\ell_j)_n^{-1}$ and the η' states as $\ell_{\eta'}$.

supported by Grants-in-Aid for Scientific Research No. 24105707 (H.N.), No. 22740161 (D.J.), and No. 24540274 (S.H.) in Japan. A part of this work was done under the Yukawa International Project for Quark-Hadron Sciences (YIPQS).

APPENDIX

In this Appendix, we show the calculated ^{12}C$(p,d)^{11}$C $\otimes\,\eta'$ spectra at $T_p = 2.5$ GeV with various combinations of the potential strength with the range of V_0 from -50 to -200 MeV and $W_0 = -5$ to -20 MeV in Fig. 8.

[1] S. Weinberg, Phys. Rev. D **11**, 3583 (1975).
[2] E. Witten, Nucl. Phys. B **156**, 269 (1979).
[3] G. Veneziano, Nucl. Phys. B **159**, 213 (1979).
[4] G. 't Hooft, Phys. Rev. Lett. **37**, 8 (1976).
[5] R. D. Pisarski and F. Wilczek, Phys. Rev. D **29**, 338 (1984).
[6] J. Kapusta, D. Kharzeev, and L. McLerran, Phys. Rev. D **53**, 5028 (1996).
[7] S. D. Bass and A. W. Thomas, Phys. Lett. B **634**, 368 (2006).
[8] V. Bernard, R. Jaffe, and U. G. Meissner, Nucl. Phys. B **308**, 753 (1988).
[9] K. Tsushima, Nucl. Phys. A **670**, 198 (2000); K. Tsushima, D.-H. Lu, A. W. Thomas, and K. Saito, Phys. Lett. B **443**, 26 (1998); K. Tsushima, D.-H. Lu, A. W. Thomas, K. Saito, and R. H. Landau, Phys. Rev. C **59**, 2824 (1999).
[10] H. Nagahiro and S. Hirenzaki, Phys. Rev. Lett. **94**, 232503 (2005).

[11] D. Jido, H. Nagahiro, and S. Hirenzaki, Phys. Rev. C **85**, 032201(R) (2012).
[12] K. Itahashi *et al.*, Letter of Intent for GSI-SIS, 2011 (unpublished); K. Itahashi, H. Fujioka, H. Geissel, R. S. Hayano, S. Hirenzaki *et al.*, Prog. Theor. Phys. **128**, 601 (2012).
[13] S. H. Lee and T. Hatsuda, Phys. Rev. D **54**, R1871 (1996).
[14] T. D. Cohen, Phys. Rev. D **54**, 1867 (1996).
[15] H. Nagahiro, M. Takizawa, and S. Hirenzaki, Phys. Rev. C **74**, 045203 (2006).
[16] T. Yamazaki, S. Hirenzaki, R. S. Hayano, and H. Toki, Phys. Rep. **514**, 1 (2012).
[17] K. Itahashi *et al.*, Phys. Rev. C **62**, 025202 (2000).
[18] K. Suzuki, M. Fujita, H. Geissel, H. Gilg, A. Gillitzer *et al.*, Phys. Rev. Lett. **92**, 072302 (2004).
[19] H. Nagahiro, S. Hirenzaki, E. Oset, and A. Ramos, Phys. Lett. B **709**, 87 (2012).
[20] E. Oset and A. Ramos, Phys. Lett. B **704**, 334 (2011).
[21] T. Csörgő, R. Vértesi, and J. Sziklai, Phys. Rev. Lett. **105**, 182301 (2010).
[22] P. Moskal *et al.*, Phys. Lett. B **474**, 416 (2000).
[23] P. Moskal *et al.*, Phys. Lett. B **482**, 356 (2000).
[24] M. Nanova, V. Metag, A. Ramos, E. Oset, I. Jaegle *et al.*, Phys. Lett. B **710**, 600 (2012).
[25] M. Nanova (CBELSA/TAPS Collaboration), Prog. Part. Nucl. Phys. **67**, 424 (2012).
[26] P. Costa, M. C. Ruivo, and Y. L. Kalinovsky, Phys. Lett. B **560**, 171 (2003).
[27] H. Toki, S. Hirenzaki, and T. Yamazaki, Nucl. Phys. A **530**, 679 (1991); S. Hirenzaki, H. Toki, and T. Yamazaki, Phys. Rev. C **44**, 2472 (1991).
[28] O. Morimatsu and K. Yazaki, Nucl. Phys. A **435**, 727 (1985); **483**, 493 (1988).
[29] H. Nagahiro, D. Jido, and S. Hirenzaki, Phys. Rev. C **80**, 025205 (2009).
[30] K. Nakayama (private communication).
[31] C. Amsler *et al.*, Phys. Lett. B **667**, 1 (2008).
[32] S. L. Belostotskii *et al.*, Sov. J. Nucl. Phys. **41**, 903 (1985).
[33] K. Nakamura, S. Hiramatsu, T. Kamae, H. Muramatsu, N. Izutsu *et al.*, Phys. Rev. Lett. **33**, 853 (1974).
[34] M. F. M. Lutz, G. Wolf, and B. Friman, Nucl. Phys. A **706**, 431 (2002); **765**, 495 (2006).
[35] J. Yamagata-Sekihara, D. Cabrera, M. J. Vicente Vacas, and S. Hirenzaki, Prog. Theor. Phys. **124**, 147 (2010).
[36] R. Muto *et al.* (KEK-PS-E325 Collaboration), Phys. Rev. Lett. **98**, 042501 (2007).
[37] D. Cabrera and M. Vicente Vacas, Phys. Rev. C **67**, 045203 (2003).
[38] T. Hatsuda and S. H. Lee, Phys. Rev. C **46**, 34 (1992).
[39] Y. Maeda, M. Hartmann, I. Keshelashvili, S. Barsov, M. Buscher *et al.*, Phys. Rev. Lett. **97**, 142301 (2006).
[40] H. Nagahiro, D. Jido, and S. Hirenzaki, Nucl. Phys. A **761**, 92 (2005).
[41] S. Barsov, I. Lehmann, R. Schleichert, C. Wilkin, M. Buescher *et al.*, Eur. Phys. J. A **21**, 521 (2004).